
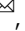





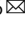


A potential collapse of the Atlantic Meridional Overturning Circulation may stabilise eastern Amazonian rainforests

Da Nian ¹, Sebastian Bathiany ², Maya Ben-Yami^{1,2}, Lana L. Blaschke ^{1,2}, Marina Hirota ^{3,4}, Regina R. Rodrigues ⁵ & Niklas Boers ^{1,2,6}

Observations and models suggest that the Amazon rainforest might transition to a savanna-like state in response to anthropogenic climate and land use change. Here, we combine observations of precipitation, temperature and tree cover with high-resolution comprehensive climate model simulations to investigate the combined effect of global warming and a potential Atlantic Meridional Overturning Circulation collapse on the Amazon. Our results show that, while strong warming lead to forest dieback, an Atlantic Meridional Overturning Circulation collapse would stabilize the Amazon by increasing rainfall and decreasing temperature in most parts. Although an Atlantic Meridional Overturning Circulation collapse would have devastating impacts globally, our results suggest that it may delay or even prevent parts of the Amazon rainforest from dieback. Besides the many negative consequences of its collapse, the interactions we identify here make a tipping cascade, i.e., that an Atlantic Meridional Overturning Circulation collapse would trigger Amazon dieback, appear less plausible.

¹Potsdam Institute for Climate Impact Research, Potsdam, Germany. ²Earth System Modelling, School of Engineering and Design, Technical University Munich, Munich, Germany. ³Group IpES, Department of Physics, Federal University of Santa Catarina, Florianópolis, Brazil. ⁴Department of Plant Biology, University of Campinas, Campinas, Brazil. ⁵Department of Oceanography, Federal University of Santa Catarina, Florianópolis, Brazil. ⁶Department of Mathematics and Global Systems Institute, University of Exeter, Exeter, UK. ✉email: danian@pik-potsdam.de; n.boers@tum.de

As the world's largest tropical forest, the Amazon rainforest is a key component of the Earth system^{1,2} and plays a large role as a carbon sink^{1,3,4} and a biodiversity hotspot. Global climate and land use changes have put the Amazon rainforest at increasing risk of dieback^{1,5–7}, which would have severe impacts on regional to global scales^{1,8–11}.

Previous studies have compared the Amazon rainforest with simple iconic dynamical systems, where small changes in a control parameter can bring the system to a bifurcation point and cause an abrupt and irreversible transition to an alternative state^{12–15}. Also some comprehensive models have suggested that the Amazon might dieback abruptly in response to the impacts of anthropogenic global warming^{16–18}.

Observations corroborate this view by showing alternative regimes of tree coverage for similar levels of mean annual precipitation¹⁹. There is therefore concern that decreasing levels of rainfall, combined with a warming-induced increase in evapotranspiration, will cause Amazon vegetation to shift into a savanna-like state from which it may not recover even when the climate forcing is reversed^{20,21}. Observations have recently indicated that the Amazon basin may indeed be approaching such a transition^{22–24}. These results agree with studies suggesting that global warming would lead to a loss of Amazon rainforest resilience²⁵, risking dieback by the end of the century^{5,26,27}. Other studies question the likelihood of the Amazon forest crossing a critical threshold^{28,29}. State-of-the-art Earth system models generally do not show large-scale dieback by the end of the twenty-first century¹⁷. However, these model projections are sensitive to parameterizations involving uncertain model parameters²¹. Moreover, a substantial number of these models show regional abrupt transitions in vegetation carbon under high-emission scenarios¹⁸. It is thus imperative to further investigate potential shifts that may occur within distinct regions of the Amazon boundaries^{5,9}.

Another key component of the Earth system⁶ is the Atlantic Meridional Overturning Circulation (AMOC). There is evidence from paleoclimate proxies and from models across the hierarchy—from conceptual models to Eddy-resolving coupled general circulation models—that the AMOC is a bistable system; there likely exists a second, substantially weaker circulation mode in addition to the present strong mode^{30–33}.

A transition of the AMOC to its weak state would result in a southward shift of the Atlantic Intertropical Convergence Zone; in turn, this has been suggested to have major impacts on rainfall regimes over the Amazon rainforest^{34–36}. Observational evidence suggests that the AMOC has already weakened in the last century and is showing signs of destabilization^{37–40}, and coupled climate models project further weakening of the AMOC under future warming⁴¹. Whilst the effects of an AMOC collapse on the South American Monsoon and the Amazon rainforests have been investigated in numerous studies^{30,34,42}, these have almost exclusively focused on the effects of a pre-industrial climate. These studies use so-called hosing experiments, in which freshwater is added to the North Atlantic, forcing the AMOC to weaken and potentially collapse.

There has been little research on the combined effect that global warming and a potential AMOC collapse would have on the Amazon rainforests. Ciemer et al.⁴³ utilized the relationship between Atlantic sea-surface temperatures and Amazon mean annual precipitation (MAP) to predict the probability of forest and savanna states on average, without an investigation of the spatial patterns. Moreover, few studies take the changes of both precipitation and temperature into account when considering future impacts.

In this work, we investigate the spatiotemporal impacts that a combined global warming and AMOC collapse scenario would

have on the Amazon rainforest. We go beyond the idealized approach in Ciemer et al.⁴³ by directly utilizing precipitation as well as temperature patterns simulated with comprehensive high-resolution Earth System Models as a response to global warming and to an AMOC collapse. To obtain the pattern of global warming in general, we use model outputs from the high-emission global warming scenario SSP5-8.5 (SSP8.5) from the sixth phase of the Climate Model Intercomparison Project (CMIP6), without restricting ourselves to the particular timing of emissions in that scenario (see “Discussion” section). The climatic changes resulting from an AMOC collapse are obtained from the North Atlantic Hosing Model Intercomparison Project (NAHosMIP)⁴⁴. In our results, we focus on the model HadGEM3-GC3-1MM (HadGEM3) because it has a relatively high resolution and high ability to simulate precipitation over Amazon⁴⁵ among the NAHosMIP models showing an AMOC collapse, but ensure that the results are similar to the model mean (see Methods) to guarantee their robustness across models.

Despite being state-of-the-art, the models employed for the above simulations do not simulate vegetation dynamically. We therefore build on the results by Hirota et al.¹⁹, in which the stability landscape of tree cover is derived from observations⁴⁶. We use satellite-derived tree cover data (Moderate Resolution Imaging Spectroradiometer (MODIS))⁴⁷ and a station-based precipitation and temperature data set (Climate Research Unit (CRU))⁴⁸ to infer probability densities of the tree cover state as function of climatic conditions. Based on these empirical relationships, we predict the shifts in tree cover distribution that would result from global warming with and without AMOC collapse.

Results

Temperature and precipitation changes in future scenarios. To study the impact of future climate change scenarios on the Amazon, we first obtain the changes in MAP and mean annual temperature (MAT) that result from either an AMOC collapse or from global warming without AMOC collapse from the different model simulations (Fig. 1). Compared with pre-industrial MAP and MAT values, the main effect of an AMOC collapse is to increase precipitation in northeastern Brazil (Fig. 1b). This increase is due to the southward shift of the Atlantic Intertropical Convergence Zone over the tropical Atlantic, which is caused by the change in meridional heat transport and the shift of the thermal equator following the AMOC collapse³⁵. The collapse also leads to a general cooling over tropical South America (Fig. 1d). In contrast, global warming results in coherent temperature increases also regionally across South America. In the SSP8.5 future emissions scenario, most areas of South America (almost the entire Amazon basin) would warm by more than 7 °C in the final decade of this century compared to pre-industrial levels (Fig. 1c). In addition, a large decrease in precipitation would occur over much of northern South America and especially the eastern half of the Amazon rainforests, while a clear increase in precipitation would occur in southern and especially southeastern South America (Fig. 1a).

Stability of the Amazon rainforest. Most studies have only considered precipitation as the environmental control parameter for tree cover^{19,20,43}. However, the increase in temperature also has relevance for the resilience of the system by increasing potential evapotranspiration, enhancing the likelihood of wildfires²⁷, and because the thermal tolerance of plants has thresholds⁴⁹. From the temperature-tree distribution projection (Supplementary Fig. S1c), it can be seen that their relationship is nonlinear. The traditional way to determine the most likely tree

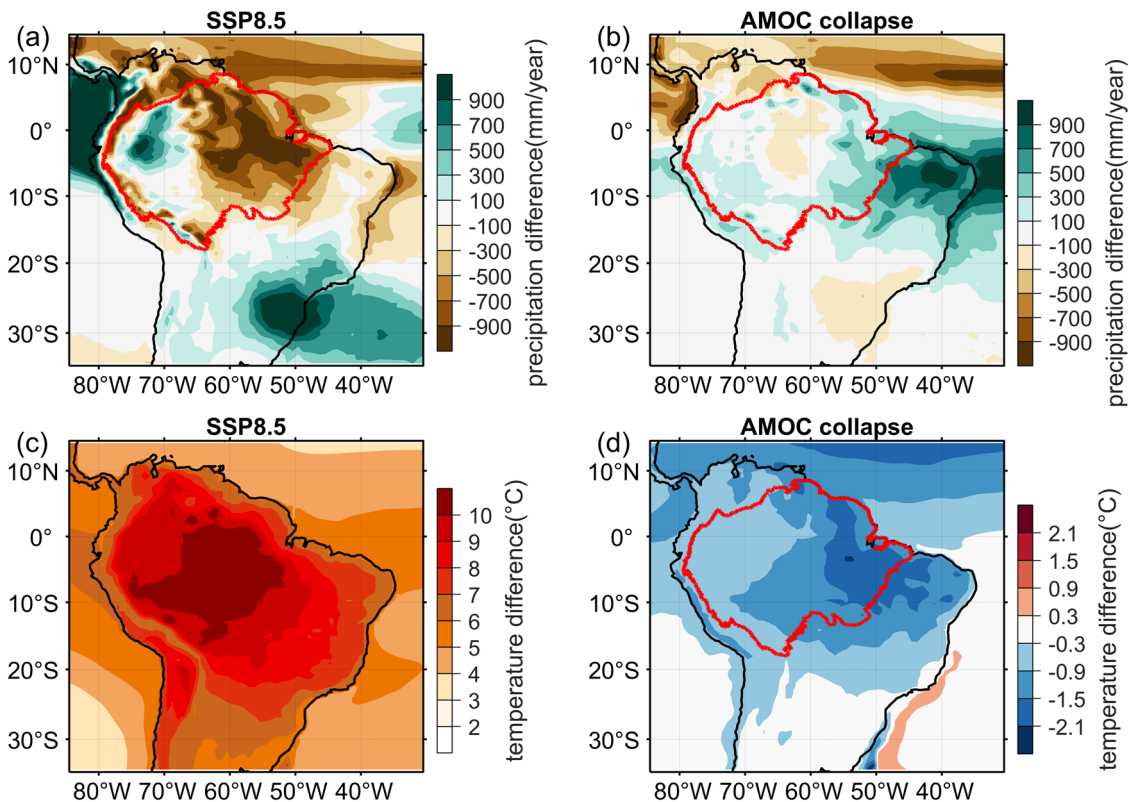


Fig. 1 Changes in precipitation and temperature due to AMOC collapse and global warming. **a** Mean annual precipitation (MAP) changes due to global warming are estimated by subtracting the mean pre-industrial control climate from the average of the final decade (2090–2100) in the SSP8.5 scenario of the HadGEM3 model. **b** Mean annual temperature (MAT) changes estimated in the same way for the SSP8.5 scenario. **c** MAP changes due to Atlantic Meridional Overturning Circulation (AMOC) collapse, estimated by subtracting the fields of the control runs from the average of the hosing experiment of HadGEM3. **d** MAT changes estimated in the same way for the AMOC collapse. The red line shows the Amazon basin, determined from http://worldmap.harvard.edu/data/geonode:amapoly_ivb.

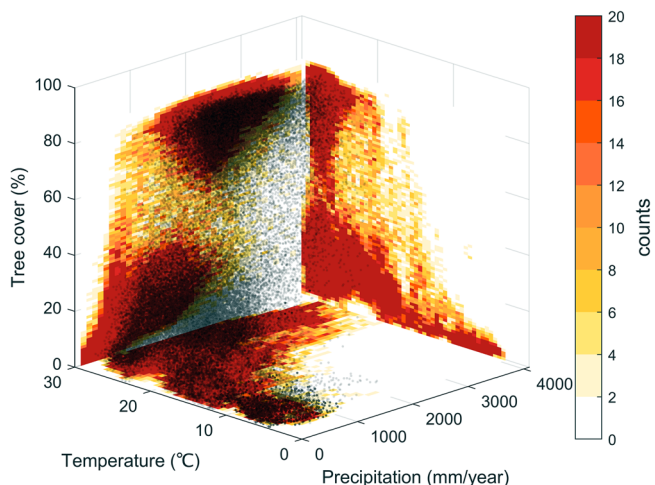


Fig. 2 Distribution of climate variables in the South America. Distribution of tree cover, mean annual precipitation (MAP), and mean annual temperature (MAT) in the study area of South America. The light gray dots are the observations from 2000 to 2020 in the three-dimensional MAP–MAT–tree-cover state space. The colored projection panels show the 2-dimensional distribution of tree cover and MAP, tree cover and MAT, as well as MAT and MAP, respectively.

cover state only considers the tree-precipitation relationship (Supplementary Fig. S1b): the tree cover distribution at a specific MAP empirically reveals forest and savanna (unimodal) as well as bistable regimes (bimodal). We therefore consider MAP and

MAT to determine the most likely tree cover state based on the empirically inferred probability density function (PDF) (Fig. 2).

As in Hirota et al.¹⁹, the observations reveal three vegetation regimes (Supplementary Fig. S2). (1) forest regime: for high MAP, forest is the only stable state. (2) Bistable regime: apart from forest, an alternative stable “savanna-like” state with low tree cover exists. This state is a non-forest state, but may have a different appearance than a typical savanna in actual observations. As MAP decreases, the forest state loses resilience in the sense that smaller disturbances are needed to cause a shift to the savanna-like state^{19,20}. (3) Savanna-like regime: for even smaller MAP, the savanna-like regime is the only remaining state with low tree coverage. We use the term “state” when we refer to the actually realized tree cover, whereas a regime is characterized by the entirety of all possible stable states.

Changes in tree cover regime in future scenarios. The impacts of climate change on the tree cover regime can be assessed by comparing the regime in the current climate to the one in future scenarios, where general model biases of course need to be taken into account. We assume that the effects of global warming and the AMOC collapse can be added linearly (see “Methods”). For any time in which a certain warming level is reached, we consider a so-called combined scenario by assuming the AMOC collapse has happened by that time. Figure 3 shows the resulting transitions of tree cover regimes in two scenarios: global warming only (SSP8.5, Fig. 3a, c, e, g), and the combined scenario (SSP8.5 + AMOC collapse, Fig. 3b, d, f, h). Note that, in addition to mean MAT and MAP changes, changes in their interannual variability—such as the effects of alterations of the El Niño Southern

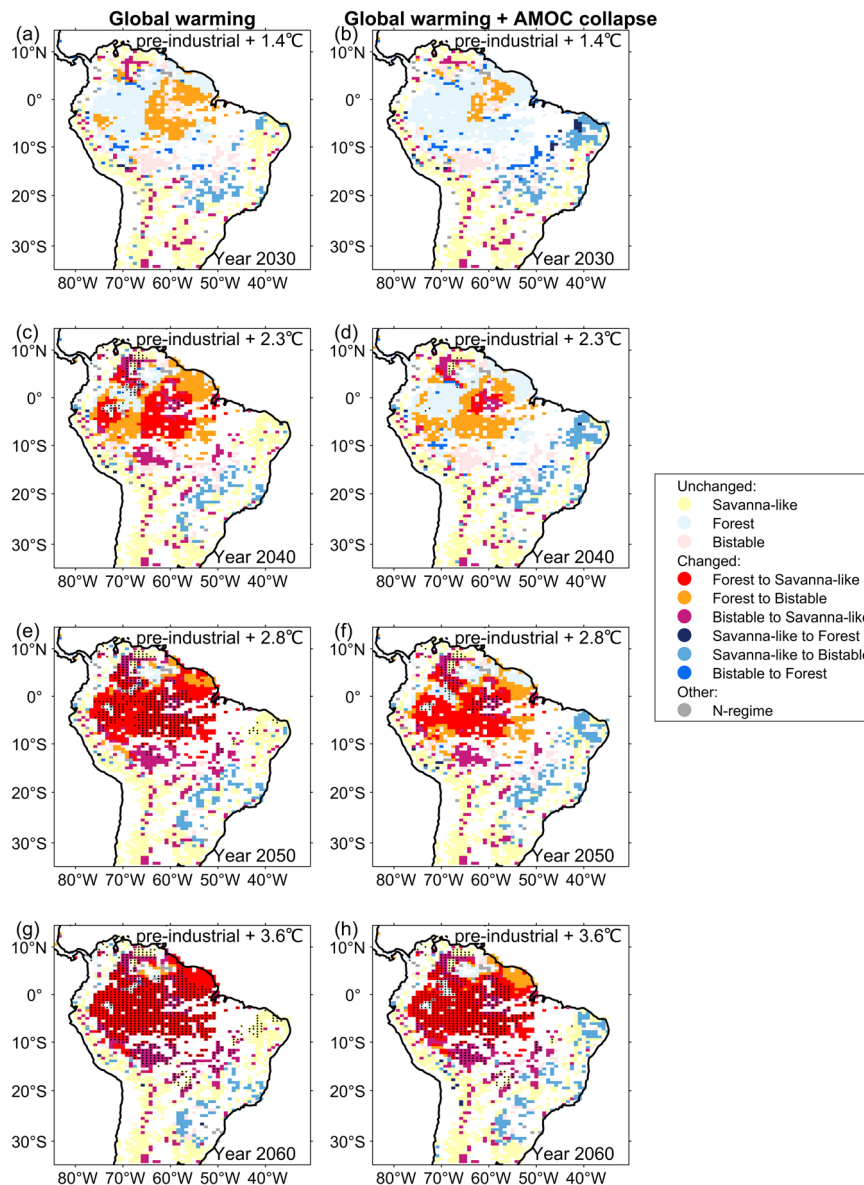


Fig. 3 Vegetation regime shifts in future scenarios. **a, c, e, g** show vegetation regime shifts in global warming (SSP8.5), and **b, d, f, h** show vegetation regime shifts in global warming combined with an Atlantic Meridional Overturning Circulation (AMOC) collapse. The global temperature changes relative to pre-industrial levels are shown at the top right corner of each panel (assuming the AMOC collapse does not affect global mean temperature). “Savanna-like, Forest, Bistable” in the color labels denote the savanna-like, forest, and bistable regime, respectively. Each color represents a vegetation regime shift, e.g., “Forest to Savanna-like” means a shift from forest to savanna-like regime (red). The “N-regime” shift shows locations for which the regimes cannot be uniquely determined (can’t tell from the PDF whether it’s monostable or bistable, see “Methods”). Black dotted areas indicate that the sample was insufficient to determine the vegetation regime from the observed relationships (No data, where mean annual precipitation (MAP) or mean annual temperature (MAT) leaves the range of observed values, see “Methods”); in particular, these include cases where MAT or MAP exit their observed range in the SSP8.5 scenario. In such cases, the result shown here is the nearest-year result with sufficient data. This figure shows that the stable forest regions in the Amazon lose resilience gradually in both future scenarios and finally transition to a stable savanna-like regime around the warming level of 3.6 °C. The resilience loss is delayed in the combined scenario compared to the SSP8.5-only situation.

Oscillation—caused by an AMOC collapse are also taken into account (“Methods”).

The results reveal that the higher the global warming level, the more likely it is that large-scale forest dieback will occur in the Amazon. The central and eastern parts of the Amazon are the first to lose resilience and undergo critical transitions from the forest to the savanna-like regime (Fig. 3a, c, e, g). This is associated with the large warming of the central Amazon and the drying occurring in eastern Amazon as shown in Fig. 1a.

The combined scenario shows a similar evolution with increasing levels of global warming (Fig. 3b, d, f, h). However,

the loss of the forest regime is shifted substantially under higher global warming levels, i.e., to later points in time. This even happens in the central Amazon, where the AMOC collapse does not increase MAP, but does decrease MAT (Fig. 1). In addition, the increased precipitation in northeastern Brazil caused by the AMOC collapse makes the forest regime more stable where it already prevails, causes transitions from the savanna-like regime to the bistable regime, and even leads to a shift from savanna-like regime to forest in some grid cells, in case the AMOC collapse occurs early enough (Fig. 3b).

Above a global warming level of 3.6 °C relative to the pre-industrial climate, more than 50% of South America would experience average temperatures beyond what is currently observed anywhere in the Amazon forest. We have insufficient data to determine the tree cover state in those situations. However, the most likely tree cover state of the overwhelming majority of these regions was already a savanna-like state prior to exceeding temperature levels covered by observations, which is indicated by the nearest-year results with sufficient data before exceeding the limits of observational records (Fig. 3). At such high temperatures the forest would face much more dry-season water stress, which in addition to the direct heat stress would cause an even higher risk of the region transitioning to a savanna-like regime²⁷.

The Amazon forest in the combined scenario reaches a critical such high temperatures the forest would face much more dry-season water stress, which in addition to the direct heat stress would cause an even higher risk of the region transitioning to a savanna-like regime transition later in time than in the SSP8.5 scenario because the AMOC collapse buffers the increasing temperatures (Fig. 1d) and increases precipitation over the eastern Amazon (Fig. 1b). This conclusion is further supported by the comparison of the spatial abundance of the three regimes (forest, savanna-like and bistable) in the two future scenarios, as shown in Fig. 4. For a global warming level below 1.4 °C above pre-industrial, the changes in MAT and MAP have relatively little impact on the abundance of the regimes. The abundance of the forest regime decreases considerably for global warming larger than 1.4 °C, whereas the area of savanna-like regime increases. Beyond 2.8 °C warming, almost the entire Amazon rainforests are at risk of dieback (Fig. 3e), though the lack of present-day analogs prevents us from predicting the threshold levels in some places. In comparison, in the combined scenario, the percentage of forest and savanna-like regime is basically stable at a relatively high value until a warming level of 2.3 °C. For higher warming levels, the percentage of savanna-like regime increases more slowly. Comparing the curves of savanna-like regime percentages, the

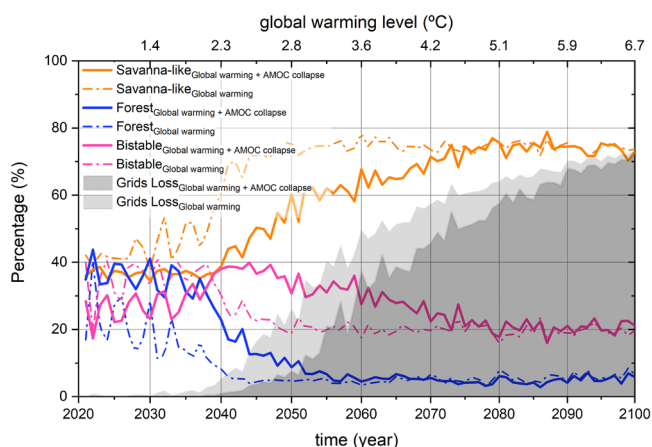


Fig. 4 Area fraction of different vegetation regimes over time. Area fraction of the savanna-like regime (orange lines), forest (blue lines), and bistable regime (pink lines) are relative to the total natural vegetation area for each year (see “Grid selection” in “Methods”). The dashed-dotted lines represent the result of the SSP8.5 simulation, and the solid lines represent the combined scenario (SSP8.5 + AMOC collapse). The gray shading indicates the area fraction of grid cells with insufficient samples at their corresponding mean annual precipitation and mean annual temperature (light gray for SSP8.5 and dark gray for the combined scenario). These grid cells are removed when estimating the percentages because the vegetation regime of these areas could not be determined.

change is delayed temporarily in the combined scenario, with good correspondence of the spatial patterns of the regime shift (Fig. 3). This indicates that even in an extreme warming scenario, a collapse of the AMOC would temporarily have a stabilizing effect on the Amazon forests.

We further demonstrate different regional impacts under the two future climate change scenarios in three regions: (1) the central Amazon, where forest resilience is lost first; (2) eastern Brazil, which substantially gains precipitation due to the AMOC collapse; and (3) a southeastern region where precipitation substantially increases due to global warming (Fig. 5a). In these regions, we follow the trajectories of regional average MAP and MAT change. In the central Amazon (Fig. 5c), MAT increases and MAP decreases steadily over time in both scenarios. The vegetation regime changes from forest to bistable, and finally to savanna-like regime. An AMOC collapse occurring in an early stage of the scenario would help maintain the stability of the forest a bit longer, mainly due to the cooling effect. However, at a later stage, the increase in MAT is too large, and the forest would turn into a savanna-like regime regardless of the scenario. In northeastern Brazil and Amazon (Fig. 5b), the large amount of precipitation brought by the AMOC collapse initially shifts the region to a bistable regime in the combined scenario. Only beyond a warming level of 3.8 °C above pre-industrial, the temperature increases to an extent that the tree cover regime reverts back to a monostable savanna-like regime. In southeastern South America (Fig. 5d), increases in precipitation and temperature lead the region to gradually change from savanna-like to bistable, and eventually to forest. For this special case, the main reason that the transition of savanna-like regime to forest can occur is the relatively low original MAT and the large precipitation increase due to the greenhouse forcing (Supplementary Fig. S3a).

Dependency on the order of events. We investigated the combined consequences of global warming in the SSP8.5 scenario and an AMOC collapse occurring in a certain year, without considering their order of occurrence. The first possibility is that in a certain future year, global warming has already led to a regime shift of the vegetation, after which an AMOC collapse induces additional—potentially favorable as we saw above—impacts on vegetation. However, due to the hysteresis and associated irreversibility, for this temporal order the AMOC collapse would have happened too late to prevent or delay forest dieback. Another possible scenario is that the AMOC collapse occurs early (i.e., at a low warming level), followed by further impacts from greenhouse forcing. In this situation, the potential for preventing or delaying forest dieback would be much greater. Because of the large uncertainty in the global warming level at which AMOC collapse could occur, both scenarios are plausible. Although the final regime shift pattern shown in (Figs. 3–5) is the same in both cases, the actually attained vegetation state in the bistable regime may be either forest or savanna-like depending on the initial state, due to the memory effect of bistable systems. Thus, tree cover in the combined scenario may differ depending on the relative timing of global warming and the AMOC collapse. We therefore compare the pattern of actual tree cover states with the AMOC collapse event occurring before or after the high-level global warming (Fig. 6), by considering the observed initial state. For example, the central Amazon rainforest is in a bistable regime already below the warming level of 2.8 °C. If the AMOC collapse occurs first, its effect on the Amazon rainforest is to stabilize the forest by increasing MAP and decreasing MAT. The effects of subsequent higher-level global warming would cause a shift from a stable forest regime to a bistable regime. With forest as the

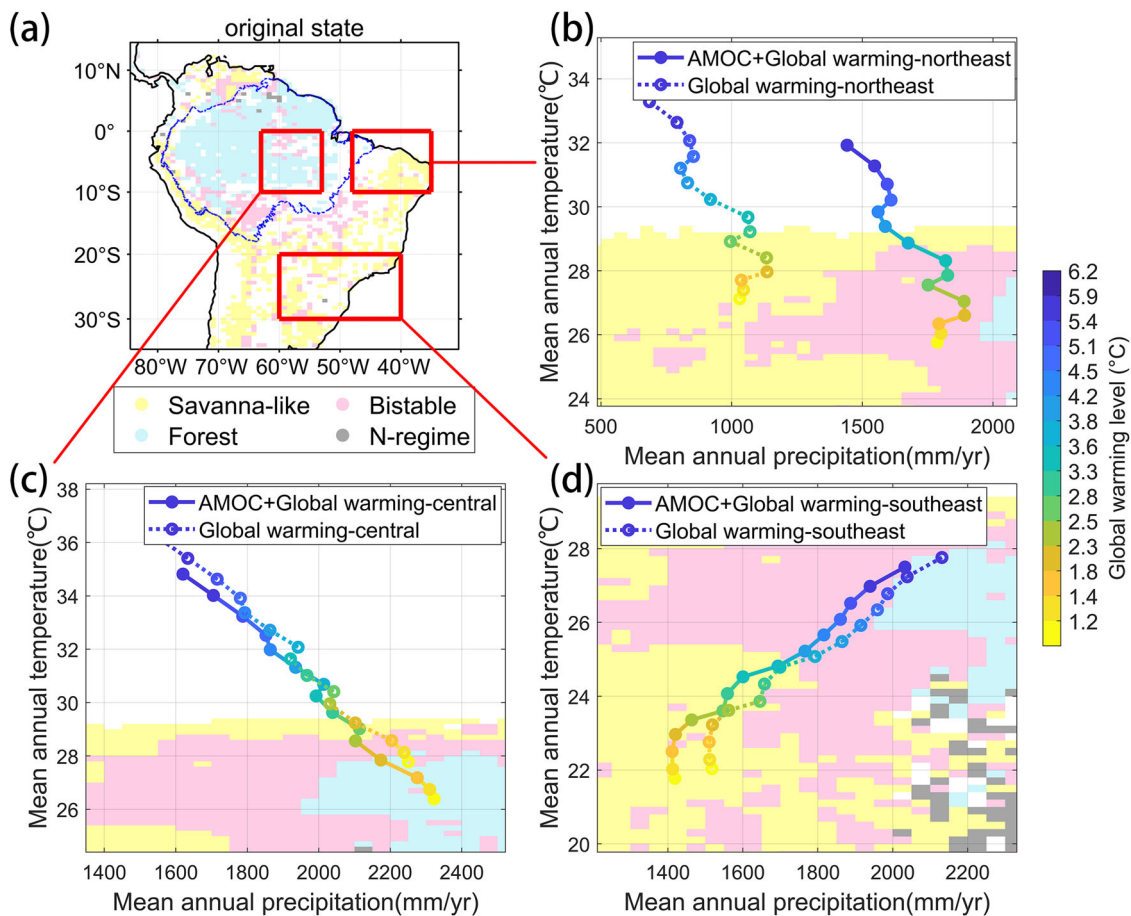


Fig. 5 Trajectories of climate change for three selected regions in two future scenarios. **a** The original tree cover state estimated from the current climate. The locations of the three regions (central: 53°W–63°W, 0–10°S; northeast: 35°W–48°W, 0–10°S; southeast region: 40°W–60°W, 20°S–30°S) are marked by red rectangles. The trajectories of the regional average mean annual precipitation (MAP) and mean annual temperature (MAT) changes in **(b)** northeastern Brazil, **(c)** the central Amazon, and **(d)** southeastern Brazil are shown respectively. Dashed lines show the trajectories of SSP8.5, and solid lines show SSP8.5 combined with an Atlantic Meridional Overturning Circulation (AMOC) collapse. The background color indicates the vegetation regime: forest, savanna-like, bistable, and N-regime (see “Methods”), estimated from the corresponding MAP and MAT for each point coordinate in the plot, and the white part in the background due to “No Data” (see “Methods”).

initial state, the system will not have crossed the tipping point and forests would eventually be preserved. In contrast, if a high level of global warming occurs first, it can cause forest dieback as the savanna-like regime is the most likely state. The decreased MAT and increased MAP that occur later due the AMOC collapse would restore the bistable regime. However, if the tree cover has already been lost by that time, this change will not be enough to restore the forest.

Discussion

This work is based on the model outputs from the HadGEM3 model, which was chosen due to its high resolution and high ability to simulate precipitation over Amazon⁴⁵. Ben-Yami et al.⁵⁰ tested HadGEM3 and three other models (CanESM5, CESM2 and IPSL-CM6A-LR) from NAHosMIP and found consistent results indicating a southward shift of the Atlantic Intertropical Convergence Zone, increased precipitation, and cooler temperatures over the specified region after AMOC collapse, which support our analysis. Similar patterns also showed in several recent studies using state-of-the-art Earth System Models (ESMs) to simulate the effects of AMOC collapse^{51–53}. To better support the HadGEM3 results, we repeated our analysis using the averaged result of hosing experiments in three other models (CanESM5, CESM2

and IPSL-CM6A-LR) with bistable AMOC in NAHosMIP⁴⁴ (see “Methods”) and the ensemble mean of 35 models in CMIP6 SSP8.5 (Supplementary Figs. S4 and S5). As the results are of considerably lower resolution, a direct comparison of results on the scale of a few 100 km is hardly possible. However, the essential large-scale features of our results, in particular the delayed forest loss in the central Amazon, remain valid. Our overall results are hence not model-dependent.

Since SSP8.5 represents the most extreme warming scenario, offering a future climate change projection across a large potential range of warming levels, including the climate response to high rates of deforestation, we have also repeated the analysis under the SSP2-4.5 scenario (SSP4.5), a medium pathway for future greenhouse gas emissions that supersedes the RCP4.5 pathway, employing the ensemble mean of 32 CMIP6 SSP4.5 models (see “Methods”). We find that the results from the SSP4.5 scenario can be scaled to match the results from the SSP8.5 scenario (Supplementary Fig. S4). For instance, the vegetation regime shift pattern shown at a global warming level of 2.1 °C in SSP8.5 for the year 2050, aligns with the year 2040 in SSP4.5 (also exhibiting 2.1 °C of warming), exhibiting a similar pattern. Also, year 2060 in SSP8.5 aligns with year 2099 in SSP4.5. The combined scenario under SSP4.5 still shows the delay effect of resilience loss compared with the SSP4.5-only situation.

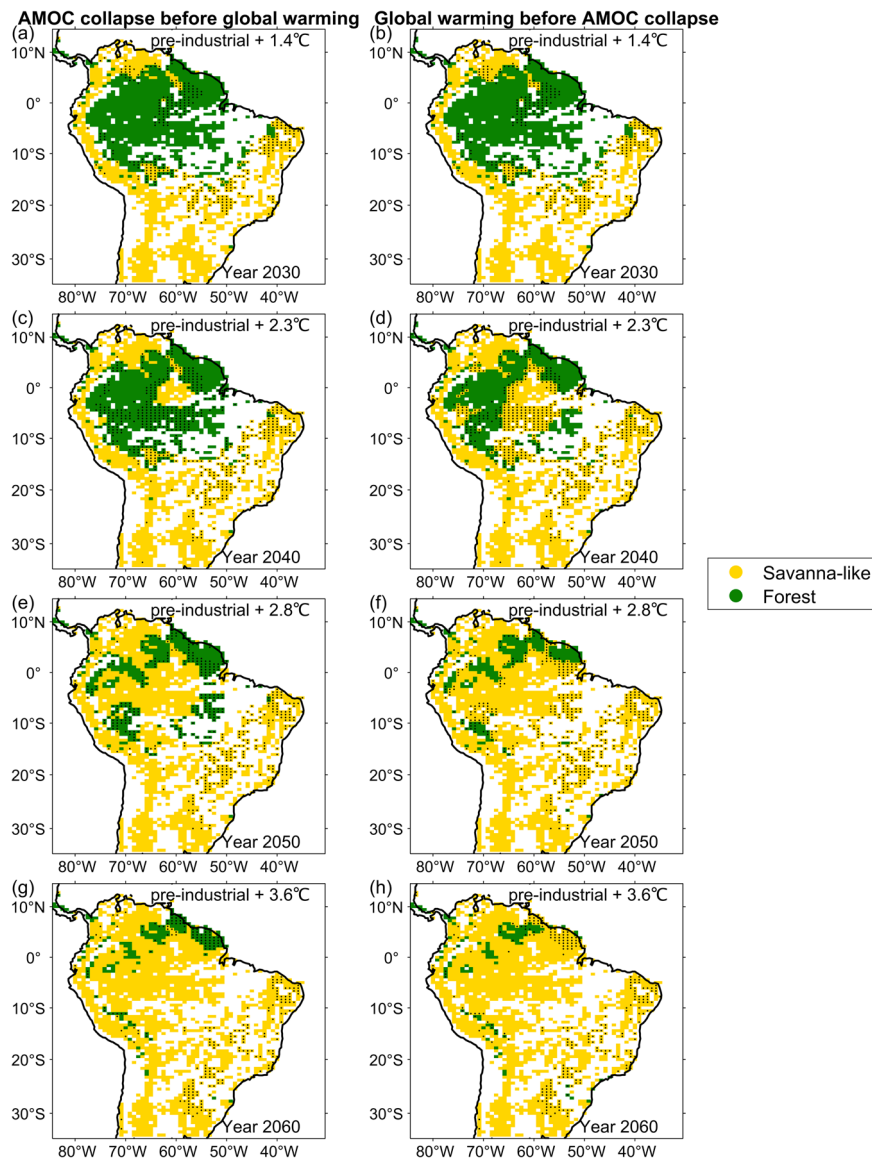


Fig. 6 Tree cover state for two future situations considering their order of occurrence. **a, c, e, g** show the tree cover state for the Atlantic Meridional Overturning Circulation (AMOC) collapse that occurs before the effects of global warming (SSP8.5) come into play. **b, d, f, h** show the tree cover state for global warming (SSP8.5) that occurs before the AMOC collapse. The shaded areas show the bistable regime.

The combined scenario in our study assumes that the MAP and MAT changes due to the SSP scenario forcing and the AMOC collapse forcing are linearly additive. The advantage of this approach lies not only in its flexibility and detailed examination of the effects of different timings of an AMOC collapse, but also in its ability to circumvent the increased uncertainties associated with predicting future collapses using Earth system models⁵⁴. This is particularly crucial given the substantial inter-model variability observed among CMIP6 models in predicting AMOC response to warming scenarios⁵⁵. The study by Chemison et al.⁵³, who applied freshwater hosing in the North Atlantic in the standard RCP8.5 scenario using the IPSL-CM5A model, shows similar precipitation and temperature changes in their results compared to ours⁵³, and similar results have been shown in other model experiments⁵⁶. This indicates the credibility of the linear superposition. Previous studies have shown that CMIP6 models under the SSP8.5 scenario already exhibit a gradual AMOC decline, and our result may hence overestimate the effect of AMOC collapse in the combined scenarios. However, this effect may be limited, as the AMOC collapse signal is noticeable

in the CMIP6 model of SSP8.5 after 2050⁴¹. At such high warming levels, our results show only few differences between the two scenarios.

In this work, the inclusion of MAT as an additional parameter goes beyond previous studies^{19,20,43} where the tree cover PDF was estimated only from the MAP, whereas we introduce another dimension of environmental conditions. The nonlinear relationships between MAT and MAP and between MAT and tree cover (shown in Supplementary Fig. S1) introduce more realistic considerations. The vegetation status cannot be determined simply by the linear change of temperature and precipitation. As the result shown in Supplementary Fig. S6, when only considering the relationship between MAP and tree cover and ignoring temperature changes, the vegetation regimes show different spatial patterns.

Our findings provide a spatial pattern of vegetation regime shifts for warming only and warming plus AMOC collapse scenarios, which has not been addressed before but is a critical contribution to offering a more comprehensive understanding of the potential impacts of global warming and AMOC collapse on

vegetation. Human land-use change and deforestation are additional factors that would influence the vegetation state over Amazonia, however, our study specifically examines the natural response of the Amazon to anthropogenic warming and we exclude regions potentially impacted by human-induced deforestation. Our findings still provide key insights into where the degrading remote effects of deforestation on untouched rainforest areas could still be attenuated by an AMOC collapse. This work does not take into account the varying length of the dry season under climate change, which would also affect the vegetation state in the Amazon Basin⁵⁷. A study based on the fifth phase of the Climate Model Intercomparison Project projections finds that the dry season in the southern Amazon will be extended by the end of the twentieth century⁵⁸. However, a large part of the most affected regions are removed in our study due to potential human deforestation. Moreover, the effect of AMOC collapse on the length of dry season remains to be further studied. Therefore, the effect of dry season changes on the Amazon forest under future climate change still needs to be explored.

We have taken into account changes in interannual variability in addition to changes of the mean precipitation and temperature changes following an AMOC collapse (The difference without considering it is shown in Supplementary Fig. S6). These inter-annual variabilities of precipitation, temperature, and fire-related tree cover changes include the impacts of changing forest fires and water use efficiency on vegetation regimes as it uses data from 2000–2020, which is reflected in the empirical relationship used in this study from MAP, MAT, and tree cover. However, it should be noted that the time required for the AMOC to collapse and for the tree cover to respond to future climate change has not been considered in this study. Our results only represent the equilibrium state of tree cover after climatic changes. Continued weakening of the AMOC would likely also influence tree cover over South America dynamically in the long term, via hydrological and thermal changes^{43,59}, causing similar patterns⁵³ as found in this study, once the AMOC has reached a weak state at a certain global warming level. The tree cover regimes we identify are, however, independent of a particular time horizon or emission scenario given a certain AMOC state and global warming level. The actual evolution of tree cover will largely depend on the relative timing of the two processes, and the possibility of an AMOC collapse per se. In case of an early AMOC tipping and a “net-zero” emission pathway thereafter, it is even conceivable that parts of the Amazon can be saved on an arbitrarily long time scale.

Recent studies have extensively explored the tipping cascade effects among subsystems of the Earth System^{6,36,59}: When a tipping element crosses its tipping point, it could trigger other tipping elements to tip over in succession. In particular, the Amazon forest is susceptible to the tipping cascade effects resulting from the AMOC^{36,60,61}. We here assess the individual and combined contributions of global warming and an AMOC collapse to future climate change, as well as comparing the impacts of different times of collapse for the AMOC. Our findings suggest that an AMOC collapse tends to stabilize the Amazon forest system overall, making the occurrence of a tipping cascade less plausible in this particular scenario.

Overall, our study confirms that high global warming levels would lead to high risks of Amazon forest dieback. It also reveals that the collapse of AMOC prior to forest dieback would stabilize the Amazon rainforest and delay the regime shift. However, if global warming continues, large parts of the Amazon forests still face high risks of dieback even with a potential AMOC collapse. Limiting the global temperature increase thus remains an urgent key priority to maintain a stable Amazon rainforest.

Methods

Observations. We study the region of South America from 15N to 35S, which includes both tropical forest and savanna-like areas. We use the satellite tree cover data at 250 m resolution from the MODIS Terra vegetation continuous fields yearly product (MOD44B.006)⁴⁷ from 2000–2020. From the high-resolution gridded dataset CRU TS v. 4.06 (Climatic Research Unit gridded Time Series)⁴⁸, which is based on weather station observations at $0.5^\circ \times 0.5^\circ$ and is available at a monthly resolution, we calculate the mean annual precipitation (MAP) and mean annual temperature (MAT) from 2000–2020.

Model outputs. To estimate the influence of an AMOC collapse, hosing experiments of the comprehensive general circulation models HadGEM3-GC3-1MM (HadGEM3), CanESM5, CESM2 and IPSL-CM6A-LR are used in this study. They are part of NAHosMIP⁴⁴, a recent intercomparison project which investigates the stability of the AMOC by comparing eight models from the sixth phase of the Climate Model Intercomparison Project (CMIP6). A constant 0.3 Sv hosing is applied over the North Atlantic for 50 years, weakening the AMOC. The AMOC remains in a stable weak state after the hosing is stopped⁴⁴. MAT and MAP changes are calculated from the last 100 years of the hosing experiments and pre-industrial control runs. The main text only focuses on the result of HadGEM3 due to its exceptionally high resolution. To determine MAT and MAP changes for future scenarios, we use the pre-industrial and historical experiment data from HadGEM3 CMIP6 (<https://esgf-node.llnl.gov/search/cmip6/>). For estimating the impact of global warming, we use data from the SSP5-8.5 (SSP8.5) experiment of HadGEM3 in CMIP6 from 2015–2100. For the multi-model results, the ensemble means of 35 CMIP6 models of SSP8.5, the ensemble means of 32 CMIP6 models of SSP4.5, pre-industrial, and historical experiments are used for the same time periods in Supplementary Figs. S4 and S5 (<https://esgf-node.llnl.gov/search/cmip6/>). All data of CMIP6 used are listed in Supplementary Table S1.

Grid selection. To focus on forest and savanna-like regimes, we exclude non-vegetated areas and human-influenced regions based on the IGBP MODIS land cover dataset⁶². We also use the Hansen forest loss dataset⁶³ to further remove areas with potential human deforestation. The resolution is downscaled to 0.12° from the 0.00025° resolution by measuring the percentage of forest loss in each grid cell. Grid cells with forest loss exceeding 5% from the Hansen dataset are removed from both observations and model simulations. Note that this removal based on the Hansen dataset includes both human and natural causes of forest loss, making it a conservative approach.

Determining tree cover regimes. We estimate the most probable tree cover regime based on MAT and MAP values for each grid cell. Tree cover samples from the observations within $\pm 0.2^\circ\text{C}$ of the target MAT and ± 50 mm/year of the target MAP for the grid cell are used to calculate the probability density function (PDF) using Gaussian kernel density estimation with a bandwidth of $b = 1.06s/n^{1/5}$, where s is the standard deviation of the samples and n is the sample size (Supplementary Fig. S2). Vegetation regimes are defined based on the characteristics of the PDF peaks. If there is only one peak, regimes are classified as monostable forest if the peak is above 70% tree cover, and monostable savanna-like if the peak is below 30% tree cover. The bistable regime is assigned when the PDF exhibits two peaks, unless the savanna-like peak lies below a tree cover of 0.005 or the difference

between the second peak and the minimum is smaller than 0.001. A special case is defined as the “Neither forest nor savanna-like nor bistable” regime (N-regime), when there is only peak between 30 and 70%. Grid cells with less than 11 data samples are marked as “No data” due to insufficient data for PDF estimation, meaning where MAT or MAP leaves the range of observed values.

For the AMOC collapse situation, we estimate the tree cover regimes from the precipitation and temperature changes by subtracting the time average of the pi-Control experiment from the time average of the 100-year hosing experiment. These regimes are then compared with the vegetation regime of the currently observed climate (2000–2020) to infer vegetation regime changes after the AMOC collapse, referred to as the “averaged method”, as shown in Supplementary Fig. S6c.

To comprehensively estimate the vegetation regime, we account for the impact of interannual variability of MAT and MAP, which can be influenced by natural climate variability such as the El Niño Southern Oscillation⁶⁴. We first estimate the joint PDF of MAT and MAP from 100-year changes of AMOC collapse with n times m bins for a grid cell, and the corresponding MAP_i and MAT_j of each bin are added to the current climate to get the final MAP and MAT of this grid cell. The corresponding tree coverage PDF_{ij} for each bin can then be determined using the same method as described earlier. Regarding the corresponding probability of each bin $P(MAP_i, MAT_j)$ as weight, we then calculate the weighted average for the tree cover PDF of all bins as the final tree cover PDF of this grid as follows:

$$PDF_{\text{final}} = \sum_{i=1, j=1}^{n, m} P(MAP_i, MAT_j) * PDF_{ij}, \quad (1)$$

where the sum of the $P(MAP_i, MAT_j)$ is 1 and $m = n = 10$. The regime estimated from this tree cover PDF is compared with the regime of the current climate to obtain the weighted average vegetation regime shift of AMOC collapse, as shown in Supplementary Fig. S6d. We refer to this as the “weighted method”, which incorporates information from temperature and natural variability. Supplementary Fig. S6 provides a comparison of regime shifts due to AMOC collapse with and without considering temperature and natural variability. In the main text, both SSP8.5-only and combined scenarios account for natural variability.

For the global warming scenario without AMOC collapse, the precipitation and temperature changes are estimated by subtracting the time average of a reference period from each year’s MAP and MAT of SSP8.5 in the period 2021 to 2100. The reference period here is the period 2000–2014 of the historical experiment followed by 2015–2020 of the SSP8.5 experiment. These changes are then added to the current climate to obtain the 2021–2100 global warming anomalies relative to pre-industrial. Combined these with the joint PDF of MAT and MAP by the 100-year pre-industrial run fluctuations (with time average removed), and then estimate the weighted-average vegetation regime shift of SSP8.5 in 2021–2100 (weighted method).

To obtain the combined scenario, we assume independence and additivity of the effects of global warming and AMOC collapse. We add the MAP (MAT) for each bin of the joint PDF of changes after the AMOC collapse to the changes of global warming relative to pre-industrial, and estimate the final MAP (MAT) for each bin. From this, we can estimate the weighted-average MAP (MAT) and weighted-average vegetation regime shift for the combined scenario of AMOC collapse with global warming in 2021–2100.

When MAT exceeds 30 °C and there are no corresponding historical observation samples, we can not update anymore. Studies show that the thermotolerance of trees declines above

40 °C^{49,65}. The climatology of the Amazon determined from 2000–2020 observations shows that the MAT over the central Amazon is >27 °C (Supplementary Fig. S7), which is the riskiest region for temperature increase.

The current-climate tree cover state is determined based on averaged tree cover from observations, with values greater than 50% defined as forest and the rest as savanna-like state. In future scenarios, the tree cover state is determined based on the vegetation regime shift. If the shift results in a transition to savanna-like or forest regime, the final tree cover state is set accordingly. If the shift results in a transition to bistable regime, the tree cover state remains the same as in the current climate. For example, if the shift shows a transition from forest to bistable regime, the final tree cover state is still classified as forest, despite the regime being bistable.

The maps presented in Figs. 1, 3, 5, 6 and S3–S7 were initially generated in this study using MATLAB 2021b⁶⁶ with the M_Map package⁶⁷.

Data availability

The data used for Fig. 4 can be found at <https://doi.org/10.5281/zenodo.10120519>. The MODIS tree cover dataset is available from <https://lpdaac.usgs.gov/products/mod44b006/>. The MODIS Land Cover dataset can be downloaded at <https://lpdaac.usgs.gov/products/mcd12c1v006/>. The precipitation and temperature dataset from CRU TS v. 4.06 can be downloaded at <https://catalogue.ceda.ac.uk/uuid/e0b4e1e56c1c4460b796073a31366980>. The CMIP6 model output datasets analyzed during this study are available online at <https://esgf-node.llnl.gov/search/cmip6/>. The NAHosMIP data are available from <https://doi.org/10.5281/zenodo.7324394>.

Code availability

The codes used for the analysis are available on request from the corresponding author.

Received: 22 May 2023; Accepted: 17 November 2023;

Published online: 12 December 2023

References

- Nobre, C. et al. (eds) *Science Panel for the Amazon. Amazon Assessment Report 2021* (United Nations Sustainable Development Solutions Network, 2021).
- Verweij, P. et al. *Keeping the Amazon Forests Standing: A Matter of Values* (WWF-Netherlands, 2009).
- Espirito-Santo, F. D. et al. Size and frequency of natural forest disturbances and the Amazon forest carbon balance. *Nat. Commun.* **5**, 1–6 (2014).
- Esquivel-Muelbert, A. et al. Tree mode of death and mortality risk factors across Amazon forests. *Nat. Commun.* **11**, 5515 (2020).
- Lovejoy, T. E. & Nobre, C. Amazon tipping point: last chance for action. *Sci. Adv.* **5**, eaba2949 (2019).
- Lenton, T. M. et al. Tipping elements in the Earth’s climate system. *Proc. Natl Acad. Sci.* **105**, 1786–1793 (2008).
- Lapola, D. M. et al. The drivers and impacts of Amazon forest degradation. *Science* **379**, eabp8622 (2023).
- Steffen, W. et al. Trajectories of the Earth system in the anthropocene. *Proc. Natl Acad. Sci.* **115**, 8252–8259 (2018).
- Canadell, J. G. et al. Global carbon and other biogeochemical cycles and feedbacks. in *Climate Change 2021: The Physical Science Basis. (Chapter in IPCC6)* (eds Masson-Delmotte, V. et al.) (Cambridge University Press, 2021).
- Lapola, D. M. et al. Limiting the high impacts of Amazon forest dieback with no-regrets science and policy action. *Proc. Natl Acad. Sci.* **115**, 11671–11679 (2018).
- Boers, N., Marwan, N., Barbosa, H. M. & Kurths, J. A deforestation-induced tipping point for the South American monsoon system. *Sci. Rep.* **7**, 41489 (2017).
- Lenton, T. M. Early warning of climate tipping points. *Nat. Clim. Change* **1**, 201–209 (2011).
- Van Nes, E. H. et al. What do you mean, ‘tipping point’? *Trends Ecol. Evol.* **31**, 902–904 (2016).
- Ditlevsen, P. D. & Johnsen, S. J. Tipping points: early warning and wishful thinking. *Geophys. Res. Lett.* **37**, L19703 (2010).

15. Scheffer, M. et al. Early-warning signals for critical transitions. *Nature* **461**, 53–59 (2009).
16. Cox, P. M. et al. Amazonian forest dieback under climate-carbon cycle projections for the 21st century. *Theor. Appl. Climatol.* **78**, 137–156 (2004).
17. Drijfhout, S. et al. Catalogue of abrupt shifts in intergovernmental panel on climate change climate models. *Proc. Natl Acad. Sci.* **112**, E5777–E5786 (2015).
18. Parry, I. M., Ritchie, P. D. & Cox, P. M. Evidence of localised Amazon rainforest dieback in CMIP6 models. *Earth Syst. Dyn.* **13**, 1667–1675 (2022).
19. Hirota, M., Holmgren, M., Van Nes, E. H. & Scheffer, M. Global resilience of tropical forest and savanna to critical transitions. *Science* **334**, 232–235 (2011).
20. Staal, A. et al. Hysteresis of tropical forests in the 21st century. *Nat. Commun.* **11**, 4978 (2020).
21. Boulton, C. A., Booth, B. B. & Good, P. Exploring uncertainty of Amazon dieback in a perturbed parameter Earth system ensemble. *Glob. Change Biol.* **23**, 5032–5044 (2017).
22. Boulton, C. A., Lenton, T. M. & Boers, N. Pronounced loss of Amazon rainforest resilience since the early 2000s. *Nat. Clim. Change* **12**, 271–278 (2022).
23. Smith, T., Traxl, D. & Boers, N. Empirical evidence for recent global shifts in vegetation resilience. *Nat. Clim. Change* **12**, 477–484 (2022).
24. Forzieri, G., Dakos, V., McDowell, N. G., Ramdane, A. & Cescatti, A. Emerging signals of declining forest resilience under climate change. *Nature* **608**, 534–539 (2022).
25. Ciemer, C. et al. Higher resilience to climatic disturbances in tropical vegetation exposed to more variable rainfall. *Nat. Geosci.* **12**, 174–179 (2019).
26. Nobre, C. A. & Borma, L. D. S. 'tipping points' for the Amazon forest. *Curr. Opin. Environ. Sustain.* **1**, 28–36 (2009).
27. Malhi, Y. et al. Exploring the likelihood and mechanism of a climate-change-induced dieback of the Amazon rainforest. *Proc. Natl Acad. Sci.* **106**, 20610–20615 (2009).
28. Chai, Y. et al. Constraining Amazonian land surface temperature sensitivity to precipitation and the probability of forest dieback. *NPJ Clim. Atmos. Sci.* **4**, 6 (2021).
29. Kukla, T. et al. The resilience of Amazon tree cover to past and present drying. *Glob. Planet. Change* **202**, 103520 (2021).
30. Henry, L. et al. North Atlantic ocean circulation and abrupt climate change during the last glaciation. *Science* **353**, 470–474 (2016).
31. Stommel, H. Thermohaline convection with two stable regimes of flow. *Tellus* **13**, 224–230 (1961).
32. Rahmstorf, S. Ocean circulation and climate during the past 120,000 years. *Nature* **419**, 207–214 (2002).
33. Jackson, L. & Wood, R. Hysteresis and resilience of the AMOC in an eddy-permitting GCM. *Geophys. Res. Lett.* **45**, 8547–8556 (2018).
34. Good, P., Boers, N., Boulton, C. A., Lowe, J. A. & Richter, I. How might a collapse in the Atlantic Meridional Overturning Circulation affect rainfall over tropical South America? *Clim. Resil. Sustain.* **1**, e26 (2022).
35. Jackson, L. et al. Global and European climate impacts of a slowdown of the AMOC in a high resolution GCM. *Clim. Dyn.* **45**, 3299–3316 (2015).
36. Wunderling, N., Donges, J. F., Kurths, J. & Winkelmann, R. Interacting tipping elements increase risk of climate domino effects under global warming. *Earth Syst. Dyn.* **12**, 601–619 (2021).
37. Boers, N. Observation-based early-warning signals for a collapse of the Atlantic Meridional Overturning Circulation. *Nat. Clim. Change* **11**, 680–688 (2021).
38. Caesar, L., McCarthy, G. D., Thornalley, D., Cahill, N. & Rahmstorf, S. Current Atlantic Meridional Overturning Circulation weakest in last millennium. *Nat. Geosci.* **14**, 118–120 (2021).
39. Caesar, L., Rahmstorf, S., Robinson, A., Feulner, G. & Saba, V. Observed fingerprint of a weakening Atlantic ocean overturning circulation. *Nature* **556**, 191–196 (2018).
40. Michel, S. L. et al. Early warning signal for a tipping point suggested by a millennial atlantic multidecadal variability reconstruction. *Nat. Commun.* **13**, 5176 (2022).
41. Weijer, W., Cheng, W., Garuba, O. A., Hu, A. & Nadiga, B. CMIP6 models predict significant 21st century decline of the Atlantic Meridional Overturning Circulation. *Geophys. Res. Lett.* **47**, e2019GL086075 (2020).
42. Parsons, L. A., Yin, J., Overpeck, J. T., Stouffer, R. J. & Malyshev, S. Influence of the Atlantic Meridional Overturning Circulation on the monsoon rainfall and carbon balance of the American tropics. *Geophys. Res. Lett.* **41**, 146–151 (2014).
43. Ciemer, C., Winkelmann, R., Kurths, J. & Boers, N. Impact of an AMOC weakening on the stability of the southern Amazon rainforest. *Eur. Phys. J. Spec. Top.* **230**, 3065–3073 (2021).
44. Jackson, L. C. et al. Understanding AMOC stability: the North Atlantic Hosing Model Intercomparison Project. *Geosci. Model Dev.* **16**, 1975–1995 (2023).
45. Firpo, M. A. F. et al. Assessment of CMIP6 models' performance in simulating present-day climate in Brazil. *Front. Clim.* **4**, 948499 (2022).
46. Staver, A. C., Archibald, S. & Levin, S. A. The global extent and determinants of savanna and forest as alternative biome states. *Science* **334**, 230–232 (2011).
47. DiMiceli, C. et al. MOD44B MODIS/Terra Vegetation continuous fields yearly L3 global 250m SIN Grid V006 [data set]. NASA EOSDIS Land Processes DAAC. <https://doi.org/10.5067/MODIS/MOD44B.006> (2015).
48. Harris, I., Osborn, T. J., Jones, P. & Lister, D. Version 4 of the CRU TS monthly high-resolution gridded multivariate climate dataset. *Sci. Data* **7**, 109 (2020).
49. Araujo, I. et al. Trees at the Amazonia-Cerrado transition are approaching high temperature thresholds. *Environ. Res. Lett.* **16**, 034047 (2021).
50. Ben-Yami, M. et al. Robust and irreversible impacts of an AMOC collapse on tropical monsoon systems: a multi-model comparison. *ESS Open Archive* <https://doi.org/10.22541/essoar.169447451.12077946/v1> (2023).
51. Orihuela-Pinto, B., England, M. H. & Taschetto, A. S. Interbasin and interhemispheric impacts of a collapsed atlantic overturning circulation. *Nat. Clim. Change* **12**, 558–565 (2022).
52. Bellomo, K. et al. Impacts of a weakened AMOC on precipitation over the Euro-Atlantic region in the EC-Earth3 climate model. *Clim. Dyn.* **61**, 3397–3416 (2023).
53. Chemison, A., Defrance, D., Ramstein, G. & Caminade, C. Impact of an acceleration of ice sheet melting on monsoon systems. *Earth Syst. Dyn.* **13**, 1259–1287 (2022).
54. Rahmstorf, S. et al. Exceptional twentieth-century slowdown in Atlantic ocean overturning circulation. *Nat. Clim. Change* **5**, 475–480 (2015).
55. Gong, X., Liu, H., Wang, F. & Heuzé, C. Of atlantic meridional overturning circulation in the cmip6 project. *Deep Sea Res. Part II Top. Stud. Oceanogr.* **206**, 105193 (2022).
56. Liu, W., Xie, S.-P., Liu, Z. & Zhu, J. Overlooked possibility of a collapsed atlantic meridional overturning circulation in warming climate. *Sci. Adv.* **3**, e1601666 (2017).
57. Hutyrá, L. R. et al. Climatic variability and vegetation vulnerability in Amazonia. *Geophys. Res. Lett.* **32**, L24712 (2005).
58. Boisier, J. P., Ciais, P., Ducharne, A. & Guimberteau, M. Projected strengthening of Amazonian dry season by constrained climate model simulations. *Nat. Clim. Change* **5**, 656–660 (2015).
59. Wunderling, N. et al. Global warming overshoots increase risks of climate tipping cascades in a network model. *Nat. Clim. Change* **13**, 75–82 (2023).
60. Lenton, T. M. et al. Climate tipping points—too risky to bet against. *Nature* **575**, 592–595 (2019).
61. Armstrong McKay, D. I. et al. Exceeding 1.5 c global warming could trigger multiple climate tipping points. *Science* **377**, eabn7950 (2022).
62. Friedl, M. & Sulla-Menashe, D. MCD12C1 MODIS/Terra+Aqua land cover type yearly L3 global 0.05Deg CMG V006. [data set]. NASA EOSDIS Land Processes DAAC. <https://doi.org/10.5067/MODIS/MCD12C1.006> (2015).
63. Hansen, M. C. et al. High-resolution global maps of 21st-century forest cover change. *Science* **342**, 850–853 (2013).
64. Marengo, J. A. Interdecadal variability and trends of rainfall across the amazon basin. *Theor. Appl. Climatol.* **78**, 79–96 (2004).
65. Tiwari, R. et al. Photosynthetic quantum efficiency in south-eastern Amazonian trees may be already affected by climate change. *Plant Cell Environ.* **44**, 2428–2439 (2021).
66. MATLAB, T. Matlab version: 9.11.0.1809720 (r2021b). <https://www.mathworks.com> (2021).
67. Pawlowski, R. M_Map: a mapping package for MATLAB: version 1.4m, (Computer software). www.eoas.ubc.ca/~rich/map.html (2020).

Acknowledgements

This is TiPES Contribution #216; the Tipping Points in the Earth System (TiPES) project has received funding from the European Union's Horizon 2020 research and innovation programme under Grant Agreement No. 820970. N.B. and S.B. acknowledge funding by the Volkswagen foundation. M.B.-Y. and N.B. have received funding from the European Union's Horizon 2020 research and innovation programme under the Marie Skłodowska-Curie grant agreement No. 956170.

Author contributions

D.N. and N.B. conceived and designed the research. D.N. conducted the analysis and wrote the first version of the manuscript. D.N., S.B., M.B.-Y., L.L.B., M.H., R.R.R. and N.B. discussed the results, drew conclusions, and edited the manuscript.

Competing interests

The authors declare no competing interests. R.R.R. is an Editorial Board Member for Communications Earth & Environment, but was not involved in the editorial review of, nor the decision to publish this article.

Additional information

Supplementary information The online version contains supplementary material available at <https://doi.org/10.1038/s43247-023-01123-7>.

Correspondence and requests for materials should be addressed to Da Nian or Niklas Boers.

Peer review information *Communications Earth & Environment* thanks Han Dolman and Rong Fu for their contribution to the peer review of this work. Primary Handling Editor: Aliénor Lavergne. A peer review file is available.

Reprints and permission information is available at <http://www.nature.com/reprints>

Publisher's note Springer Nature remains neutral with regard to jurisdictional claims in published maps and institutional affiliations.



Open Access This article is licensed under a Creative Commons Attribution 4.0 International License, which permits use, sharing, adaptation, distribution and reproduction in any medium or format, as long as you give appropriate credit to the original author(s) and the source, provide a link to the Creative Commons licence, and indicate if changes were made. The images or other third party material in this article are included in the article's Creative Commons licence, unless indicated otherwise in a credit line to the material. If material is not included in the article's Creative Commons licence and your intended use is not permitted by statutory regulation or exceeds the permitted use, you will need to obtain permission directly from the copyright holder. To view a copy of this licence, visit <http://creativecommons.org/licenses/by/4.0/>.

© The Author(s) 2023